Transport of biomass burning products from Siberian wildfires into the Arctic

Transport of biomass burning products from Siberian wildfires into the Arctic

S A Sitnov[1] **and I I Mokhov**[1, 2]

[1] Obukhov Institute of Atmospheric Physics, Russian Academy of Sciences, Moscow, Russia
[2] Lomonosov Moscow State University, Moscow, Russia

E-mail: [1]sitnov@ifaran.ru

Abstract. The study of the long-range transport of biomass burning products from Siberian wildfires into the Arctic atmosphere during the period of 2000-2019 is presented. An analysis of the characteristics of forest fires over the past 20 years revealed an increase in radiation power of an average Siberian wildfire, which is characterized by a statistically significant linear trend of 1.7 ± 1.0% / year. A joint analysis of fire activity in Siberian forests, as well as the contents of the black carbon (BC) and carbon monoxide (CO) contents in the Arctic atmosphere, indicates that extreme fire events force the development of regional anomalies in BC and CO. Correlation between the anomalies of BC (CO) over the Russian segment of the Arctic and the number of Siberian wildfires is found to be statistically significant at the $\alpha = 0.05$ level and reach the value $r = 0.77$ (0.48) during the summer months. Using a linear regression model, an estimate of the sensitivity of changes in the total BC content and in the volume mixing ratio of CO at the 700-hPa level in the $1.9 \cdot 10^{-8}$ kg·m^{-2} per 1000 fires and 0.4 ppbv per 1000 fires, respectively. The results of a detailed analysis of the long-range BC transport into the Arctic during catastrophic Siberian wildfires in the summer of 2019 are presented. It is shown that the considered episode was conditioned by the features of the large-scale atmospheric circulation characteristic for the atmospheric blocking event.

1. Introduction

With the ongoing global warming, climatic changes in the Arctic are attracting special attention [1,2]. The increase in the average annual near-surface temperature in the Arctic latitudes during last decades is several times higher than the average temperature rise over the planet (so called Arctic amplification) [3,4]. An additional factor contributing to the heating of the Arctic system under global warming is the BC content in the air, which is a component of the submicron aerosol of the atmosphere, which effectively absorbs solar radiation [5]. When deposited on snow-covered and ice surfaces, BC reduces the albedo and increases the absorption of solar radiation, contributing to additional heating of the underlying surface [6].

Among the sources of BC in the atmosphere are anthropogenic and natural factors, associated with incomplete fuel combustion [7]. On the territory of Russia, the main source of BC during the warm period of the year is massive wildfires, which are responsible for more than 80% of the total BC emission [8], moreover the wildfires in Western Siberia and Eastern Siberia account for 23% and 50% of the total number of forest fires in Northern Eurasia [9]. In recent years, there has been a positive trend in the radiation power of an "average" Russian fire of 0.48 W m-2 per year in magnitude [9]. According to model estimates, with the continuation of global warming in the XXI century, in the

Asian part of Russia one should expect an increase in the frequency of wildfires [10] and an increase in the duration of the fire hazardous period.

Due to the small number of local sources, the main regulator of the BC content in the Arctic atmosphere is the processes of long-range transport of BC [11. The transport of pollution from middle latitudes to the Arctic is often associated with atmospheric blocking events. It was shown that seasonal variations in the concentration of anthropogenic aerosol over Arctic Alaska are associated with seasonal variations in the frequency and position of mid-latitude blocking anticyclones [12]. The rapid (7-10 days) transport of aerosols from the south to the north occurs over the western periphery of quasi-stationary anticyclones.

The aim of this work is to analyze the connection of pollution of the Arctic atmosphere by BC and CO with the Siberian forest fires, as well as to analyze possible physical mechanisms of long-range transport of biomass combustion products from Siberia to the Arctic.

2. Data

The characteristics of Siberian wildfires are analyzed using measurements from MODIS satellite instruments operated on board of the Terra and Aqua platforms from November 2000 to December 2020 with a reliability of fire diagnosis of not less than 80%. MODIS Active Fire Products (C6, L2), processed by standard MCD14ML algorithm are obtained through the FIRMS (Fire Information for Resource Management System, https://earthdata.nasa.gov) system. A detailed description of the fire detection algorithm MODIS C6 and its differences from previous one can be found in [13].

Hourly BC column mass densities (M2T1NXAER v5.12.4) and BC surface mass concentrations (M2T1NXAER v5.12.4) as well as 10-m northward wind (M2T1NXSL v.5.12.4 10M) from the MERRA-2 reanalysis were used. MERRA-2 (Modern-Era Retrospective analysis for Research and Applications, version 2) is a modern reanalysis, created in NASA with an emphasis on assimilation of various satellite measurements since 1980. MERRA-2 uses the new version of the GEOS-5 (Goddard Earth Observing System model, version 5) data assimilation system to synthesize regular time series of gridded data with a spatial resolution 0.5° x 0.625° (latitude x longitude) at 72 pressure levels (from the surface to 0.01 hPa) both instantaneous and time-averaged (hourly, 3-hourly and monthly). Among the advantages of MERRA-2, in comparison with its previous version, is joint assimilation of aerosol and meteorological fields with accounting their interaction through the radiative effects of atmospheric aerosol [14].

The daytime measurements of the CO mole fraction in air (AIRS3STM_006_CO_VMR_A) obtained by high-resolution spectrometer AIRS (Atmospheric InfraRed Sounder, C6) were also used. AIRS operates onboard the Aqua satellite from September 2002. It measures radiation in 2378 IR channels (3.7-15.4 μm) and 4 channels in the visible range (0.4-1 μm) using measurements near a wavelength of 4.6 μm for the CO retrieval . The accuracy of AIRS CO measurements is 15%, the spatial resolution in the nadir is 13.5 km, while the vertical resolution is 1 km [15]. BC and CO data were obtained through the Giovanni Internet server https://giovanni.gsfc.nasa.gov/giovanni developed and maintained by the NASA Goddard Earth Science Information Technology Information Center [16.

In addition, the geopotential heights at 500-hPa level (H500) taken from the NCEP/NCAR reanalysis [17] were used. Daily mean data of H500 with a spatial resolution of 2.5° × 2.5° were obtained from the https://www.esrl.noaa.gov/psd/data/gridded/data.ncep.reanalysis.html server.

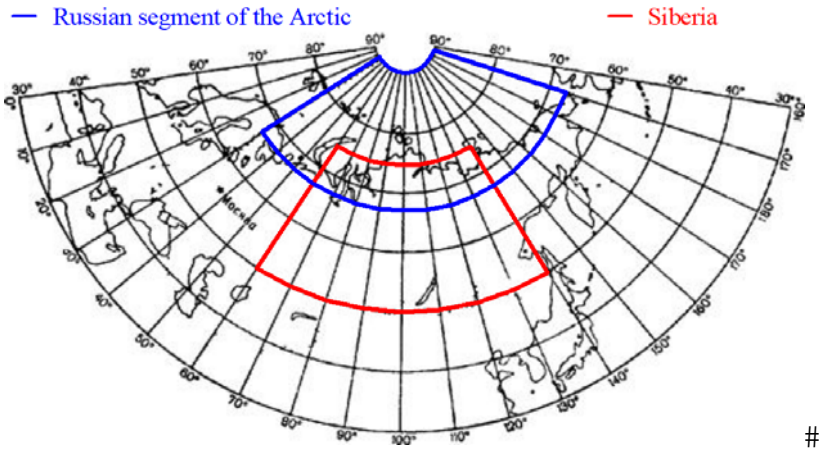

Figure 1. Territories of Siberia and the Russian segment of the Arctic considered in this study.

3. Method

The paper analyzes the relationship between the content of BC and CO in the atmosphere over the territory restricted by coordinates 66°-90°N, 30°-180°E (hereinafter the Russian segment of the Arctic) with wildfires detected in the area bounded by coordinates 50°-75°N, 60°-140°E (hereinafter Siberia) (figure 1). The regions under consideration are territories close in location. The area of the Russian segment of the Arctic is 9.2 million km^2, the area of the considered territory of Siberia is 11.3 million km^2.

4. Results and discussion

4.1. Siberian forest fires

The results of the analysis of hotspots detected by MODIS instruments indicate a regular manifestation of fire activity in Siberian forests with a strong interannual and intra-annual variability of forest fires. Formally, the regional amount of wildfires in Siberian forests (N) and the total fire radiation power (FRP) are characterized by weak positive linear trends. However, the calculations of the coefficients of variation N and FRP ($C_V = \sigma / \mu$) show that C_V exceeds 100%, which indicates on inhomogeneity of the data and makes it impossible to obtain statistically valid characteristics from the analyzed samples, including estimates of trends in N and FRP.

On the other hand, monthly variations of the ratio of the total FRP to the total fire counts are characterized by a much lower value of C_V (19%), which allows a statistical analysis of the data (figure 2a). The ratio is an estimate of the radiation power of the average Siberian fire (FRP_{avg}). Analysis of FRP_{avg} variations during the summer periods of 2003 - 2019 shows that the radiation power of the average Siberian fire is characterized by a noticeable increase, which can be approximated by a positive linear trend of 1.25 ± 0.82% / year, which is statistically significant at the α= 5% level (trend is calculated in % of the average value of FRP_{avg} in 2003-2019). The results obtained confirm the trend of an increase in the radiation power of the Siberian wildfire, obtained earlier on the basis of the analysis of shorter time series [9].

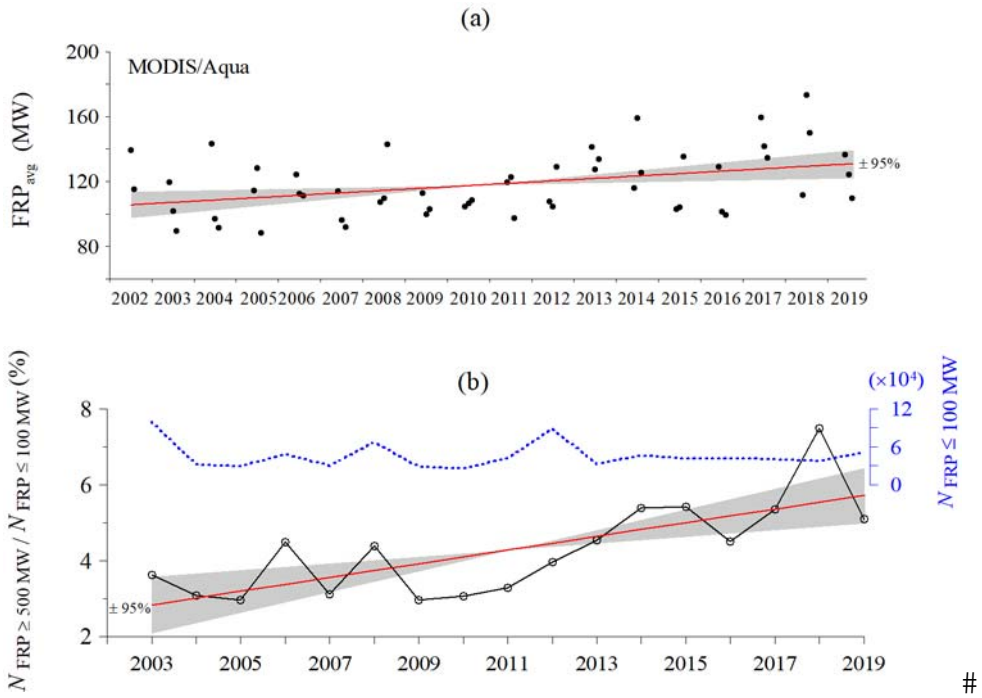

Figure 2. (a) - Yearly variations of FRP_{avg} of the average Siberian wildfire in June-August during the period of 2002-2019 and its linear trend (red line) with a 95% confidence interval (shaded area); (b) - the ratio of the number of intense fires (FRP ≥ 500 MW) to the number of weak fires (FRP ≤ 100 MW) (black line) and its linear trend (red line) with a 95% confidence interval (shaded area).Variations in the number of weak fires (blue dashed line, right scale) are also shown. MODIS/Aqua data.

The total mass of forest fires is dominated by hotspots characterized by a low FRP [9]. At the same time in [9] it was shown that from west to east in Russia the frequency of weak wildfires decreases while the frequency of intense forest fires increases. It is of interest to analyze the tendencies of long-term changes in Siberian wildfires of various intensities. figure 2b shows the annual variations in the ratio of the number of summer wildfires in Siberia with an intensity of more than 500 MW and those less than 100 MW. The results obtained indicate that in the last two decades, in the territory of Siberia, there has been a predominant increase in the number of intense forest fires, characterized by a statistically significant linear trend of 1.8 ± 0.9% / 10 years. It is characteristic that long-term changes in the number of summer Siberian fires with a FRP of less than 100 MW does not show any pronounced tendencies (figure 2b).

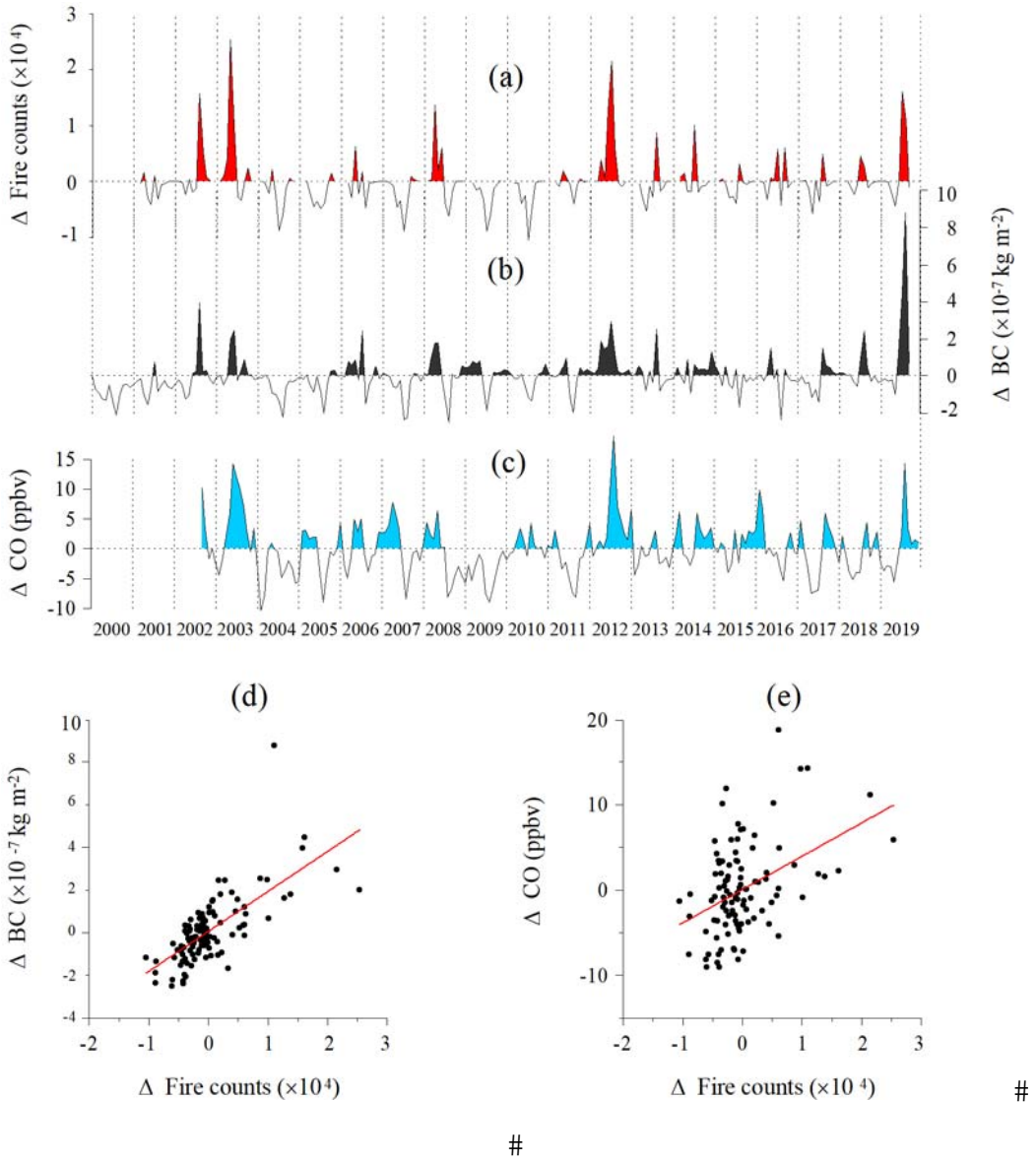

Figure 3. Monthly variations in the number of Siberian wildfires (a) and also monthly variations in the BC column density (b) and in CO VMR at 700 hPa (c) in the Arctic atmosphere. Scatter plots between Siberian wildfires and BC column density in the Arctic (d) and between Siberian wildfires and CO VMR at 700 hPa in the Arctic (e). The data sets in (a-c) were deseasonalized by subtraction of the long-term monthly means from the time-series. The scatter plots show relations between the anomalies in the fire hazardous periods (Apr-Sept).

4.2. Relationship of the BC and CO anomalies in the Arctic atmosphere with Siberian wildfires

figure 3a shows the differences between the current monthly number of Siberian wildfires and corresponding long-term monthly mean values, which characterize the anomalies of fire activity in the forests of Siberia. Calculated in a similar way the monthly mean BC and CO anomalies in the atmosphere over the Russian segment of the Arctic are shown in figure 3b and figure 3c, respectively. Comparison of figure 3a and figure 3b indicates that the increased fire activity in the forests of Siberia, noted in August 2002, May 2003, April 2008, June-July 2012 and in July-August 2019 (figure 3a), was accompanied by positive anomalies of the BC content in the Arctic atmosphere (figure 3b). The

correlation of the monthly BC anomalies in the Arctic with the number Siberian wildfires in the period 2001-2019 reaches r = 0.70 (95% confidence interval: 0.62, 0.77), and moreover increases in the summer period to r = 0.77 (0.64, 0.86). Because the contextual algorithm of MODIS detects fires in ground pixels with a size of 1 km × 1 km, the total number of fires is at the same time an lower estimate of their total area. The high correlation between BC ond wildfires is explained by a relationship between the emission of biomass burning products with the total area of wildfires [18]. The direct relationship between the Arctic BC anomalies and Siberian wildfires is confirmed by the scatter diagram (figure 3d). Figure 3d shows that the increase of BC is associated with an increase in wildfire activity in Siberian forests. Obtained on the basis of a linear regression model the estimate of the sensitivity of changes in the BC column mass density over the Russian segment of the Arctic to changes in the number of wildfires in Siberia, is 1.9 10^{-8} kg·m^{-2}/1000 wildfires.

Comparison of figure 3a and figure 3c indicates that increased fire activity in Siberian forests in 2003, 2012, and 2019 was also accompanied by positive CO anomalies in the Arctic troposphere (figure 3c). The correlation of the monthly mean values of CO anomalies in the Arctic with the number of fires in Siberia in the period 2002-2019 is r = 0.39 (0.26, 0.51), increasing in the summer period to r = 0.48 (0.24, 0.67). A weaker correlation of CO with wildfires (in comparison with BC) can be associated with a greater variety of CO sources in the Russian sector of the Arctic. The results indicate, in particular, the manifestation of positive CO anomalies in winter, as well as in early spring and late autumn, i.e. outside the fire hazardous season (see figure 3c). This fact can be associated with anthropogenic influence. The longer lifetime of CO in the atmosphere (from several weeks to several months) increases the contribution of long-range CO transport from urban territoriest in the formation of regional CO anomalies. The weaker relationship between CO in the Arctic atmosphere and forest fires in Siberia is also confirmed by the scatter diagram (figure 3f). The sensitivity of CO changes in the troposphere of the Arctic to changes in the number of fires in Siberia, obtained on the basis of a linear regression model, was estimated to be 4.0·10^{-4} ppbv / 1000 wildfires.

4.3. Mechanism of the long-range transport of biomass burning products from Siberian wildfires into the Arctic atmosphere

When considering the Russian territory as a whole, the relation of massive forest fires with atmospheric blockings was found in a number of papers [19-21]. An analysis of the topography of geopotential heights of the 500-hPa pressure level (H500) showed that episodes of extreme fire activity in Siberian forests (figure 3a) were associated with large-scale circulation characteristic for atmospheric blockings (not shown due to lack of space). Atmospheric blockings contribute to the formation of regional anomalies of atmospheric impurities, including CO, aerosol, ozone (with the formation of mini-ozone holes) [19-25].

The results of a detailed analysis of the long-range transport of BC into the Arctic during severe forest fires in Siberia in the first ten days of August 2019 are presented in figures 4.The episode under consideration was accompanied by the formation of the most strong positive BC anomaly over the Russian segment of the Arctic during the period of 2001-2019 (comp. figure 3a and figure 3b).

An analysis of longitudinal-temporal variations in the blocking index (figure 4b), calculated according to [26], indicate the manifestation of atmospheric blocking in the longitudinal sector 95°-125°E in the first ten days of August 2019. The spatial distribution of H500 (figure 4a) in this period was characterized by a stationary high-pressure system situated over the central part of Siberia (60°N, 110°E), and two stable low-pressure systems located over the Northern Urals and the Far East. The noted features of H500 are characteristic for the large-scale atmospheric circulation during atmospheric blocking event. An analysis of fire activity indicates that atmospheric blocking in the first ten days of August 2019 was accompanied by the development of massive fires in Siberian forests (figure 4e). A joint analysis of wildfires and H500 reveal that the bulk of the sources of air pollution by biomass burning products were concentrated in the center of the blocking area (figure 4a).

The mechanism of long-range transport of pyrogenic pollutants in August 2019 is closely related to atmospheric blocking. Figure 4a indicates that when approaching the blocking anticyclone, the

western zonal flow deviated far to the north, and when bending around it, to the south, dragging the air contaminated with combustion products with it. Since the spatial gradient of H500 to the west of the anticyclone exceeded the gradient of H500 to the east (figure 4a), the wind speed over the western periphery of the anticyclone was higher than the wind speed over its eastern periphery. Therefore, in a whole, the blocking area was dominated by the flow of combustion products from the south to the north, i.e. from the territory of forest fires to the Arctic.

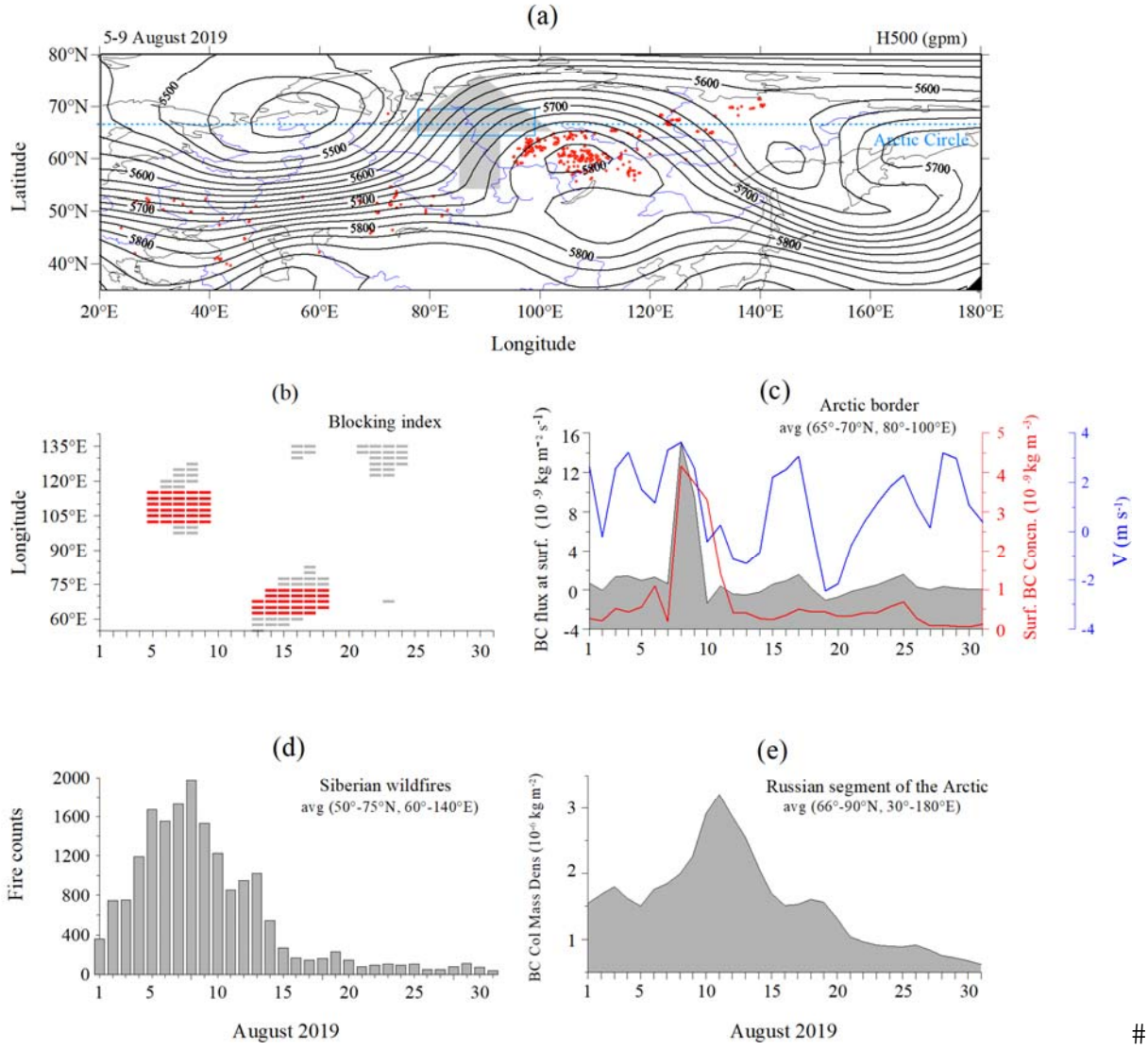

Figure 4. (a) - Spatial distributions of H500 (black isolines) and wildfires (red circles) during 5-9 August 2019, daily variations of: (b) - blocking index (red symbols stand for blocking conditions lasting at least 5 days), (c) - meridional BC flux in the surface layer through the Arctic Circle (shaded); BC mass concentration (red line) and meridional wind at the 10-m height (blue line) in the surface layer close to the Arctic Circle (see also (a)), (d) , the number of Siberian wildfires, (e) - BC total column over the Russian segment of the Arctic. In (a) blue rectangle denotes territory considered in (c), thick arrow shows the northward flux of burning products.

As part of the work, an estimate of the BC fluxes from wildfires in Siberia into the Arctic atmosphere was obtained. For calculations, the formula was used:

$$F_{BC} = C_{BC} \cdot V,$$

where F_{BC} - is the BC flux through the Arctic Circle (AC) [kg m^{-2} s^{-1}], C_{BC} - is the surface BC mass concentration [kg m^{-3}], V - is the meridional wind at the height of 10-m [m s^{-1}].

Figure 4c shows the day-to-day variations in the meridional flux of BC, regional BC mass concentration and meridional wind in the atmospheric surface layer on August 2019. All data are averaged over the spatial region (66°-69°; 80°-100°E) centered on the Arctic Circle (AC) (see also figure 4a). In early August, due to not enough developed wildfires, even despite the strengthening of the southerly wind, a weak BC flux to the Arctic was noted near the AC. It can be seen from figure 4c that at the end of the first ten days of August, forest fires in Siberia reached their maximum development, that has saturate subarctic atmosphere by combustion products. The followed strengthening in the southerly wind over the southern boundary of the Arctic, led to a sharp increase in the BC flux to the Arctic, which reached its maximum value of $1.5 \cdot 10^{-8}$ kg m^{-2} on 8 August 2019. At the beginning of the second decade of August, a decrease in the number of fires and a change in wind from south to north led to a weakening and even reversal of the BC flux, contributing to a decrease in the regional BC concentration in Arctic (figure 4e). The subsequent strengthening of the southerly wind led to a slight increase in the BC flux to the Arctic due to a significant decrease in the number of forest fires in the Siberian forests (figure 4d).

Changes in the total BC content in the atmosphere over the Russian sector of the Arctic (figure 4e) indicate an increase in the regional atmospheric BC abundance in the first ten days of August 2019, which has reached the maximum of $3.21 \cdot 10^{-8}$ kg m^{-2} on 11 August 2019. The three-day delay exists between the maximum of BC content in the Arctic for and the maximum of BC flux over AC, which can be explained by the time required for the BC transport from forest fires in Siberia into the Arctic.

5. Conclusion

The conducted analysis of the causes and mechanisms of the formation of large-scale anomalies in BC and CO contents in the atmosphere of the Russian sector of the Arctic revealed a direct relationship of the regional BC and CO anomalies with forest fires in Siberia. The estimates of the sensitivity of changes in the regional content of aircraft and CO in the atmosphere of the Russian Arctic to the corresponding changes in the number of Siberian fires were obtained: $1.9 \cdot 10^{-8}$ kg m^{-2} / 1000 fires and $4.0 \cdot 10^{-4}$ ppbv / 1000 fires, respectively.

The analysis of fire activity in Siberian forests showed that in the last two decades, there has been a predominant increase in the number of intense forest fires, characterized by a statistically significant linear trend of 1.8 ± 0.9% / 10 years (figure 2a), while long-term changes in the number of weak forest fires reveal no somehow trend.

A detailed analysis of extreme BC pollution of the high-latitude atmosphere during catastrophic forest fires in Siberia in the summer of 2019 reveals that regional pequliarities of large-scale atmospheric circulation asociated with atmospheric blocking event contributed to the long-range transport of BC from the fires of the Siberian forests to the Arctic. Estimates of BC flux from Siberian forest fires through the Arctic circle into the Arctic have been were obtained. The maximum BC flux in August 2019 reached the value of $1.5 \cdot 10^{-8}$ kg m^{-2} s^{-1}.

Acknowledgements

This work was carried out with the financial support of a project of the Russian Federation represented by the Ministry of Science and Higher Education of the Russian Federation (agreement No. 075-15-

2020-776) using results of regional analysis of blocking effects, obtained within the framework of project 19-17-00240 of the Russian Science Foundation.

References

[1] *Climate Change 2013: The Physical Science Basis*. Contribution of Working Group I to the Fifth Assessment Report of the Intergovernmental Panel on Climate Change ed T Stocker et al (New York: Cambridge University Press) pp 659–740
[2] Serreze M C, Barrett A P, Stroeve J C, Kindig D N and Holland M M 2009 The emergence of surface-based Arctic amplification *Cryosphere* **3** 11-19
[3] Screen J A, Deser C and Simmonds 2012 I Local and remote controls on observed Arctic warming *Geophys. Res. Lett.* **39** L10709
[4] Mokhov I I 2020 Russian climate research in 2015–2018 *Izvestiya, Atmos Oceanic Phys.* **56** (4) 325-343
[5] Haywood J M and Boucher O 2000 Estimates of the direct and indirect radiative forcing due to tropospheric aerosols: A review *Rev. Geophys*. **38** 513–43
[6] Hansen J and Nazarenko L 2003 Soot climate forcing via snow and ice albedos *Proc. Natl. Acad. Soc. USA*. **101** 423-28
[7] Bond T C, Doherty S J, Fahey D W, Forster P M, Berntsen T, DeAngelo B J, Flanner M G, Ghan S,. Kärcher B, Koch D et al 2013 Bounding the role of black carbon in the climate system: A scientific assessment *J. Geophys. Res. Atmos.* **118** 5380–552
[8] Evans M, Kholod N, Kuklinski T, Denysenko A, Smith S J, Staniszewski A, Hao W M, Liu L and Bond T C 2017 Black carbon emissions in Russia: A critical review *Atmos. Environ.* **163** 9-21
[9] Sitnov S A and Mokhov I I 2018 A comparative analysis of the caracteristics of active fires in the boreal forests of Eurasia and North America based on satellite data *Izv., Atmos. Oceanic Phys.* **54** 966–78
[10] Mokhov I I and Chernokulsky A V 2010 Regional model assessments of the risk of forest fires in the Asian part of Russia under climate changes *Geogr. Prir. Resur.* **2** 120–126
[11] Vinogradova A A, Smirnov N S, Korotkov V N and Romanovskaya A A 2015 Forest fires in Siberia and the Far East: Emissions and atmospherict transport of black carbon to the Arctic *Atmos. Oceanic Optics* **28** . 566-74
[12] Iversen T and Joranger E 1985 Arctic air pollution and large scale atmospheric flows *Atmos. Environ.*, **19**, 2099–108
[13] Giglio L, Schroeder W and Justice C O 2016 The collection 6 MODIS active fire detection algorithm and fire products *Rem. Sens. Environ*. **178** 31-41
[14] Gelaro R, McCarty W J, Suarez M J, Todling R, Molod A, Takacs L, Randles C A, Darmenov A, Bosilovich M G, Reichle R et al 2017 The modern-era retrospective analysis for research and applications, Version 2 (MERRA-2) *J. Clim.* **30** 5419–54
[15] Aumann H H, Chahine M T, Gautier C, Goldberg M D, Kalnay E, McMillin L M, Revercomb H, Rosenkranz P W, Smith W L et al 2003 AIRS/AMSU/HSB on the Aqua mission: Design, science objectives, data products, and processing systems *IEEE Trans. Geosci. Remote Sens*. **41** 253-264
[16] Acker J C and Leptoukh G 2007 Online analysis enhances use of NASA Earth science data *Eos Trans. AGU* **88** 14-17
[17] Kistler R, Collins W, Saha S, White G, Woollen J, Kalnay E, Chelliah M, Ebisuzaki W, Kanamitsu M, Kousky V et al 2001 The NCEP-NCAR 50-year reanalysis: Monthly means CD–ROM and documentation *Bull. Amer. Meteor. Soc*. **82** 247-268
[18] Bondur V G, Gordo K A and Kladov V L 2017 Spacetime distributions of wildfire areas and emissions of carbon-containing gases and aerosols in northern Eurasia according to satellite-monitoring data *Izv. Atmos. Ocean. Phys*. **53** 859-874

[19] Bondur V G, Mokhov I I, Voronova O S and Sitnov S A 2020 Satellite monitoring of Siberian wildfires and their effects: Features of 2019 anomalies and trends of 20-year changes *Dokl. Earth Sci.* **492** 370–375
[20] Mokhov I I, Bondur V G, Sitnov S A and Voronova O S 2020 Satellite monitoring of wildfires and emissions into the atmosphere of combustion products in Russia: Relation to atmospheric blockings *Dokl. Earth Sci.* **495** 921–24
[21] Mokhov I I, Sitnov S A, Tsidilina M N and Voronova O S 2021 NO_2 emission into the atmosphere from forest fires in Russia in relation with atmospheric blocking event *Atmos. Oceanic Optics* **34** (in press)
[22] Peters D, Egger J, Entzian G 1995 Dynamical aspects of ozone mini-hole formation *Meteorol. Atoms. Phys.* **55** 205-214
[23] James P M 1998 A climatology of ozone miniholes over the Northern Hemisphere *Int. J. Climatol.* **18** 1287–1303
[24] Barriopedro D, Anto M, Garcia J A 2010 Atmospheric blocking signatures in total ozone and ozone miniholes *J. Climate* **23** 3967-3983
[25] Sitnov S A, Mokhov I I 2015 Ozone mini-hole formation under prolonged blocking anticyclone conditions in the atmosphere over European Russia in summer 2010 *Dokl. Earth Sci.* **460** (1) 41-45
[26] Tibaldi S and Molteni F 1990 On the operational predictability of blocking *Tellus* **42A** 343-365